Published in final edited form as:
Eur J Neurosci. 2014 March ; 39(5): 771–787. doi:10.1111/ejn.12439.

Connexin36 in gap junctions forming electrical synapses between motoneurons in sexually dimorphic motor nuclei in spinal cord of rat and mouse

W. Bautista and **J. I. Nagy***
Department of Physiology, Faculty of Medicine, University of Manitoba, Winnipeg, Canada

Abstract

Pools of motoneurons in lumbar spinal cord innervate sexually dimorphic perineal musculature and are themselves sexually dimorphic, displaying differences in numbers and size in male *vs*. female rodents. In two of these pools, the dorsomedial nucleus (DMN) and the dorsolateral nucleus (DLN), dimorphic motoneurons are intermixed with non-dimorphic neurons innervating anal and external urethral sphincter (EUS) muscles. As motoneurons in these nuclei are reportedly linked by gap junctions, we examined immunofluorescence labelling for the gap junction-forming protein connexin36 (Cx36) in male and female mouse and rat. Fluorescent Cx36-puncta occurred in distinctly greater abundance in the DMN and DLN of male rodents than observed in other spinal cord regions. These puncta were localized to motoneuron somata, proximal dendrites and neuronal appositions, and were distributed either as isolated or large patches of puncta. In both rat and mouse, Cx36-puncta were associated with nearly all (> 94%) DMN and DLN motoneurons. The density of Cx36-puncta increased dramatically from postnatal day 9 to 15, unlike developmental decreases of these puncta observed in other CNS regions. In females, Cx36-puncta in DLN was similar to that in males, but was sparse in the DMN. In EGFP-Cx36 transgenic mice, motoneurons in the DMN and DLN were intensely labelled for EGFP reporter in males, but less so in females. The results indicate the presence of Cx36-containing gap junctions in the sexually dimorphic DMN and DLN of male as well as female rodents, suggesting coupling of not only sexually dimorphic but also non-dimorphic motoneurons in these nuclei.

Keywords

gap junctions; motoneurons; EGFP-Cx36 reporter; immunofluorescence

Introduction

Clusters of intercellular channels spanning the extracellular space create gap junctions at close plasma membrane apposition between neurons, and provide the basis for electrical transmission or electrical coupling (Bennett, 1997) as well as for the cell-to-cell passage of small molecules, which can be visualized as dye-coupling after intracellular injection of tracers. The channels are formed by particular members of the family of mammalian gap junction-forming connexin proteins (Evans & Martin, 2002) that are selectively expressed in neurons, and include connexin45 (Cx45) and connexin57 (Cx57), which are highly expressed in retina (Hombach *et al*., 2004; Kamasawa *et al*., 2006; Ciolofan *et al*., 2007), and connexin36 (Cx36), which is widely expressed in subpopulations of neurons in most major brain regions (Condorelli *et al*., 2000; Sohl *et al*., 2005; Meier & Dermietzel, 2006).

*Address for correspondence: James I. Nagy, Department of Physiology, Faculty of Medicine, University of Manitoba, 745 Bannatyne Ave, Winnipeg, Manitoba, Canada R3E 0J9, nagyji@ms.umanitoba.ca, Tel. (204) 789-3767, Fax (204) 789-3934.

Although long known to be of critical physiological relevance in the CNS neural circuitry of lower vertebrates (Bennett & Goodenough, 1978), the prevalence and functional importance of electrical coupling between neurons in mammalian brain has gained general acceptance only in the last decade or so. A key feature endowed by electrical transmission among ensembles of coupled neurons is synchronization of their subthreshold membrane oscillations, which promotes recruitment of synchronous activity when threshold for firing is reached (Bennett &, Zukin, 2004; Connors & Long, 2004; Hormuzdi *et al*., 2004). Such synchronous activity is emerging as a hallmark of information processing in neuronal networks (Singer, 1999; Deans *et al*., 2001; LeBeau *et al*., 2003; Whittington & Traub, 2003; Senkowski *et al*., 2008).

The discovery of Cx36 expression in neurons (Condorelli *et al*., 1998; Söhl *et al*., 1998), demonstrations of its occurrence in ultrastructurally-identified neuronal gap junctions in adult rodent brain (Nagy *et al*., 2004), and reports of functional deficits in Cx36 knockout (ko) mice (Söhl *et al*., 2004) were among some of the factors contributing to current understanding of electrical synapses in mammalian CNS. It is likely, however, that many more Cx36-expressing neurons remain to be identified, which will be aided by immunohistochemical localization of Cx36 and by the development of transgenic mice expressing reporter proteins driven by the Cx36 promoter (Degen *et al*., 2004; Wellershaus *et al*., 2008; Helbig *et al*., 2010). We have found that Cx36 protein is rarely detectable intracellularly in neurons *in vivo*, but rather is visualized exclusively as punctate labelling (Cx36-puncta) localized to neuronal plasma membranes. Because these Cx36-puncta are reflective of the localization of neuronal gap junctions, as indicated by correlative immunofluorescence and ultrastructural analysis of immunolabelling for Cx36 (Rash *et al*., 2000,2001a,b,2004,2007a,b; Kamasawa *et al*., 2006; Li *et al*., 2008), immunolocalization of Cx36 reveals sites of electrical synapses between neurons. Among the CNS areas in which we have examined Cx36 immunolocalization, few display the striking density and patterns of Cx36-puncta that we now report in sexually dimorphic motor nuclei of the spinal cord.

These nuclei are termed sexually dimorphic because the development and maintenance of their constituent motoneurons in males is dependent on adequate levels of circulating androgens, and because these neurons in females are far fewer and smaller in size (Breedlove & Arnold, 1980; Jordan *et al*., 1982; Sengelaub & Arnold, 1986; Breedlove, 1986; Sengelaub & Forger, 2008). An additional feature of these motoneurons is their linkage by gap junctions, as reported in adult male rats (Matsumoto *et al*., 1988,1989; Coleman & Sengelaub, 2002), which is in contrast to other motoneuronal populations that are electrically coupled early during postnatal development, but loose this coupling by the end of the second postnatal week (Arasaki *et al*., 1984; Fulton *et al*., 1980; Walton & Navarette, 1991; Bou-Flores & Berger, 2001). While coupling between the dimorphic motoneurons was suggested to be mediated by gap junctions composed of Cx32 (Matsumoto *et al*., 1991,1992), we found no evidence for Cx32 expression in these motoneurons, which instead expressed Cx36, as reported in preliminary form elsewhere (Bautista *et al*., 2013a). Here, we provide a more comprehensive immunofluorescence analysis of Cx36 association with these motoneurons, and we describe the distribution of these neurons in transgenic mice in which EGFP serves as a reporter for Cx36 expression.

Materials and methods

Animals and antibodies

A total of thirty-eight mice and rats were used in the present study, consisting of the following animals of specified age, sex, transgenic and treatment groups: Normal male Sprague-Dawley rats at adult age (n = 12), postnatal day (PD) nine (n = 3) and PD fifteen (n = 3); normal adult male C57BL/6-129SvEv wild-type mice (n = 6) and transgenic Cx36

knockout mice (n = 2); normal adult female Sprague-Dawley rats (n = 3); adult male castrated (n = 3) and sham (n = 3) operated rats; transgenic adult male (n = 3) and female (n = 3) mice in which Cx36 expression is normal and bacterial artificial chromosome provides EGFP expression driven by the Cx36 promoter, designated EGFP-Cx36 mice. Colonies of the C57BL/6-129SvEv wild-type and Cx36 ko mice (Deans *et al*., 2001) were established at the University of Manitoba through generous provision of breeding pairs of these mice from Dr. David Paul (Harvard). The EGFP-Cx36 mice were taken from a colony of these mice established at the University of Manitoba starting with breeding pairs obtained from UC Davis Mutant Mouse Regional Resource Center (Davis, CA, USA; see also http://www.gensat.org/index.html). Tissues from some of these animals were taken for use in parallel unrelated studies. Animals were utilized according to approved protocols by the Central Animal Care Committee of University of Manitoba, with minimization of the numbers animals used. Experiments were carried out in accordance with The Code of Ethics of the World Medical Association (Declaration of Helsinki), printed in the British Medical Journal (18 July 1964).

Immunofluorescence labelling in this study was conducted with a total of five primary antibodies, used in various combinations. Anti-Cx36 antibodies were obtained from Life Technologies Corporation (Grand Island, NY, USA) (formerly Invitrogen/Zymed Laboratories), and those used included two rabbit polyclonal antibodies (Cat. No. 36-4600 and Cat. No. 51-6300) and one mouse monoclonal antibody (Cat. No. 39-4200). These anti-Cx36 antibodies were incubated with tissue sections at a concentration of 1-2 μg/ml. Anti-peripherin developed in chicken was obtained from Millipore (Temecula, CA, USA) and used at a dilution of 1:500 to detect peripherin protein as a marker of motoneurons (Clarke *et al*., 2010). A monoclonal anti-EGFP developed in rabbit (Cat. No. G10362) was obtained from Life Technologies Corporation and used at a concentration of 1-2 μg/ml to immunolabel EGFP in sections from EGFP-Cx36 mice. A polyclonal antibody against vesicular glutamate transporter-1 (vglut1) developed in guinea pig was obtained from Millipore and used at a dilution of 1:1000 to label vglut1-containing axon terminals in the spinal. An polyclonal goat anti-choline acetyltransferase (ChAT) antibody was obtained from Millipore and used at a dilution of 1:300 to immunolabel cholinergic motoneurons in the spinal cord.

Various secondary antibodies used included Cy3-conjugated goat or donkey anti-mouse and anti-rabbit IgG diluted 1:600 (Jackson ImmunoResearch Laboratories, West Grove, PA, USA), AlexaFlour 488-conjugated goat or donkey anti-rabbit, anti-mouse and anti-guinea pig IgG used at a dilution of 1:600 (Molecular Probes, Eugene, OR, USA), AlexaFluor-647 conjugated goat anti-chicken IgG used at a dilution of 1:500 (Life Technologies Corporation), and Cy3-conjugated goat anti-chicken used at a dilution of 1:600 (Jackson ImmunoResearch Laboratories). All primary and secondary antibodies were diluted in 50 mM Tris-HCl, pH 7.4, containing 1.5% sodium chloride (TBS), 0.3% Triton X-100 (TBSTr) and 10% normal goat or normal donkey serum.

Tissue preparation

All animals were euthanized with an overdose of equithesin (3 ml/kg), placed on a bed of ice, and perfused transcardially with cold (4°C) pre-fixative consisting of 50 mM sodium phosphate buffer, pH 7.4, 0.1% sodium nitrite, 0.9% NaCl and 1 unit/ml of heparin. The prefixative was administered at a volume of 20 ml per 100 g body weight, and was adjusted accordingly for animals in this study weighing 25 g to 300 g. For experiments involving immunohistochemical detection of Cx36, which required weak fixation for adaquate labelling of Cx36, pre-fixative perfusion was followed immediately by perfusion with fixative solution containing cold 0.16 M sodium phosphate buffer, pH 7.4, 0.2% picric acid

and either 1% or 2% formaldehyde prepared freshly from depolymerized paraformaldehyde. Volumes of fixative given ranged from 100-200 ml per 200 g body weight, again adjusted for the body weight of animals used. Typically, greater volumes were used at 1% fixative and lower volumes at 2% fixative. For experiments involving immunohistochemical detection of EGFP, which required strong fixation for labelling of EGFP, the pre-fixative perfusion was followed by perfusion with fixative solution containing cold 0.16 M sodium phosphate buffer, pH 7.4, 0.2% picric acid and 4% formaldehyde. As our standard immunohistochemical protocol often excludes a step involving postfixation of extracted tissues, after both 1-2% or 4% fixative perfusions, animals were perfused with a cold solution containing 10% sucrose and 25 mM sodium phosphate buffer, pH 7.4, to wash out fixative thereby reducing extent of tissue fixation. Spinal cords were removed and stored at 4°C for 24-48 h in cryoprotectant containing 25 mM sodium phosphate buffer, pH 7.4, 10% sucrose, 0.04% sodium azide. Sections of spinal cord were cut at a thickness of 10-15 μm using a cryostat and collected on gelatinized glass slides. Slide-mounted sections could be routinely stored at -35 °C for several months before use.

Immunofluorescence procedures

Slide mounted sections were removed from storage, air dried for 10 min, washed for 20 min in TBSTr, and processed for immunofluorescence staining, as previously described (Li *et al*., 2008; Bautista *et al*., 2012; Curti *et al*., 2012). With the weak 1-2% formaldehyde fixations employed, sections mounted on gelatinized slides occasionally have poor adherence to slides and tend to float off during processing. In such instances, this was prevented by fixation of rehydrated slide-mounted sections in 1% formaldehyde for 15, 30 or 60 seconds. For double or triple immunolabelling, sections were incubated simultaneously with two or three primary antibodies for 24 h at 4°C. The sections were then washed for 1 h in TBSTr and incubated with appropriate combinations of secondary antibodies for 1.5 h at room temperature. Some sections processed for double immunolabelling were counterstained with either green Nissl fluorescent NeuroTrace (stain N21480) or Blue Nissl NeuroTrace (stain N21479) (Molecular Probes, Eugene, OR, USA). All sections were coverslipped with the antifade medium Fluoromount-G (SouthernBiotech, Birmingham, AB, USA), and were either viewed immediately or were stored at −20 °C until taken for examination. Control procedures involving omission of one of the primary antibodies with inclusion of the secondary antibodies used for double and triple labelling indicated absence of inappropriate cross-reactions between primary and secondary antibodies for all of the combinations used in this study.

Immunofluorescence was examined on a Zeiss Axioskop2 fluorescence microscope and a Zeiss 710 laser scanning confocal microscope, using Axiovision 3.0 software or Zeiss ZEN Black 2010 image capture and analysis software (Carl Zeiss Canada, Toronto, Ontario, Canada). Data from wide field and confocal microscopes were collected either as single scan images or z-stack images with multiple optical scans capturing a thickness of 4 to 12 μm of tissue at z scanning intervals of 0.4 to 0.6 μm. Images of immunolabelling obtained with Cy5 fluorochrome were pseudo colored blue. Final images were assembled using CorelDraw Graphics (Corel Corp., Ottawa, Canada) and Adobe Photoshop CS software (Adobe Systems, San Jose, CA, USA). Movie files of 3D rendered images were created using Zeiss ZEN Black 2010 software (Carl Zeiss Canada).

Results

Sexually dimorphic motor nuclei and nomenclature

Sexually dimorphic motor nuclei at lower lumbar levels were identified, in part, according to the spinal cord atlas of Watson *et al*. (2009) as well as from descriptions of motoneurons in

these nuclei retrogradely labelled from the pudendal nerve and their target muscles (Schroder, 1980; McKenna and Nadelhaft, 1986). These nuclei in rodents are distributed at the L5-L6 levels in the spinal cord ventral horn, and their constituent motoneurons collectively innervate groups of striated muscles located in the pelvic floor. The dimorphic motor nuclei and the muscles they innervate include: i) The dorsolateral nucleus (DLN), which occupies a position in the ventrolateral corner of the ventral horn, and innervates the ischiocavernosus muscle as well as striated muscle forming the external urethral sphincter around the neck of the urinary bladder; and ii) The dorsomedial nucleus (DMN) (a.k.a., spinal nucleus of the bulbocavernosus), which is located near midline beneath the central canal at the apex and flanking the dorsolateral portions of the ventral funiculus, and innervates the bulbospongiosus (a.k.a., bulbocavernosus) muscle, as well as striated muscle forming the external anal sphincter; iii) A less prominent ventral nucleus (VN), which is located midway between the DLN and DMN at the ventral margin of the ventral horn, innervates the pelvic diaphragm or pelvic floor muscle (Thor and De Groat, 2010), and is only weakly dimorphic (Mckenna and Nadelhaft, 1986); and iv) A larger retrodorsolateral nucleus (RDLN), which is located in the lateral part of the ventral horn and dorsal to the DLN, and innervates plantar foot muscles (Nicolopoulos-Stournaras and Iles, 1983; Zuloaga *et al*., 2007).

Four points regarding nomenclature are of note; First, the DMN is also often referred to as the spinal nucleus of the bulbocavernosus (SNB) (Breedlove, 1986), but we use the term DMN here to be consistent with reference to the spinal cord location of the other nuclei examined. Second, motoneurons in the DMN are often said to innervate the bulbocavernosus and levator ani muscles (Sengelaub and Forger, 2008), but a convincing case has been made for considering the levator ani as part of the bulbospongiosus muscle complex (McKenna and Nadelhaft, 1986), which is consequently the nomenclature we use here. Third, on historical grounds and to avoid confusion, we use the term external urethral sphincter to refer to striated muscles associated with the urethra, but recognize that the more anatomically accurate term urethral rhabdosphincter is becoming convention (Thor and Groat, 2010). And fourth, although RDLN motoneurons are sometimes referred to as being sexually non-dimorphic (McKenna and Nadelhaft, 1986; Coleman and Sengelaub, 2002), RDL motoneurons innervating the intrinsic foot muscle flexor digitorum brevis have been reported to exhibit male/female differences, albeit small, that are used to define sexual dimorphism (Leslie *et al*., 1991), and are therefore referred to here as dimorphic.

Cx36 in sexually dimorphic motor nuclei of male rat and mouse

An overview of the locations of the dimorphic nuclei at L5-L6 in adult rat, with labelling for peripherin and Cx36, is presented bilaterally at low magnification in Figure 1, where peripherin is shown pseudo colored sky blue for better visualization of the nuclear groups (Fig. 1), or deep blue allowing better visualization of Cx36-puncta (red) against peripherin-positive motoneurons (Fig. 1B-E). Immunolabelling for vglut1 in combination with Cx36 and peripherin is also shown (Fig. 1C-E) to provide a comparison of Cx36/vglut1 relationships in the dimorphic nuclei *vs*. Cx36 association with vglut1-containing primary afferent terminals that we have observed at most other spinal levels (Bautista *et al*., 2013b), where vglut1 is localized largely in terminals of primary afferent origin (Alvarez *et al*., 2004). Indeed, sexually dimorphic motoneurons were reported to receive a paucity of primary afferent innervation (Jankowska *et al*., 1978; Taylor *et al*., 1982; McKenna and Nadelhaft, 1986; Thor and de Groat, 2010), and scarce vglut1-containing terminals among tightly clustered motoneuronal somata in the dimorphic nuclei (discussed below) proved to be another convenient means of locating these nuclei.

As seen in transverse sections, the somata of motoneurons in the dimorphic motor nuclei were either packed tightly together forming compact globular clusters, as in the DMN and DLN (Fig. 1A-E), or were dispersed such as those in the VN group (Fig. 1A,B). The RDLN displayed a mixture of both dispersed (Fig. 1A) and clustered (Fig. 1D) motoneurons along its rostrocaudal dimensions, with the former located caudally and the latter located rostrally. Compared with scattered Cx36-puncta observed in areas of intermediate lamina of spinal cord (Fig. 1B), immunofluorescence labelling for Cx36 was consistently more intense in some of the dimorphic nuclear groups, and immunolabelling was organized in patterns distinctly different than observed at other spinal locations. In general, labelling of Cx36 was robust in the DMN and DLN (Fig. 1B-E), moderate in the VN (Fig. 1B), and ranged from sparse in regions of the RDLN containing dispersed motoneurons (Fig. 1A,C) to moderate in those regions containing motoneurons that were more clustered (Fig. 1D).

Immunolabelling of Cx36 in the DMN and DLN was also examined in horizontal sections of rat (Fig. 2A,B) and mouse (Fig. 2C,D) spinal cord, where a greater expanse of these nuclei can be visualized in their rostro-caudally oriented columns. As previously described (Schroder, 1980; Ueyama *et al*., 1987), motoneurons in the DMN tended to be organized in intermittent clusters straddling the apex of the ventral funiculus (Fig. 2A), with the bulbospongiosus and anal sphincter motoneurons completely intermingled within these clusters (Rose and Collins, 1985; McKenna and Nadelhaft, 1986). The horizontal view more clearly revealed the remarkable density of Cx36-puncta associated with individual motoneuronal somata and their proximal dendrites within these clusters. Also more evident is the extent to which dendrites from these clusters cross the midline and form bundles of intermingled dendrites emerging from opposite sides (Rose and Collins, 1985). These bundles were typically laden with Cx36-puncta (Fig. 2A), consistent with the possibility of electrical coupling between motoneurons having contralaterally projecting dendrites, as previously suggested (Coleman and Sengelaub, 2002; see however Foster and Sengelaub, 2004). In the DLN, motoneurons are more tightly packed in both rostrocaudal and mediolateral dimensions of the nucleus (Fig. 2B1). However, in rat, medially located motoneurons innervating ischiocavernosus muscles were previously reported to be somewhat segregated from more laterally located motoneurons innervating urethral sphincter muscles (Mckenna and Nadelhaft, 1986). Punctate immunolabelling for Cx36 was distributed throughout the DLN, and appeared to consist of both small and relatively larger Cx36-puncta (Fig. 2B2). There were no discernible differences in density or size of Cx36-puncta associated with motoneurons in the medial vs. lateral half of this nucleus (Fig. 2B2). Similar results were obtained in horizontal sections through the DMN (Fig. 2C) and DLN (Fig. 2D) of mouse spinal cord. In both rat and mouse, it appeared from visual inspection that the vast majority, if not all, motoneurons in these two nuclei were invested with Cx36-puncta on their somata and/or initial dendrites, suggesting that in each nuclei, both sexually dimorphic and non-dimorphic (i.e., bulbospongiosus and anal sphincter in the DMN; ischiocavernosus and urethral sphincter in the DLN) are gap junctionally coupled. This was supported by quantitative estimates where, in images such as those in Figure 2, we counted the number of peripherin-positive motoneurons that displayed or lacked Cx36-puncta on their somata, or initial dendrites where these could be followed back to somata. In three rats, counts of a total of 566 motoneurons in DMN and 1027 in DLN revealed that 98% of motoneurons in each of these motor nuclei had associated with them at least a few, but often many, Cx36-puncta. In three mice, counts of 98 motoneurons in the DMN and 206 neurons in the DLN showed that 94% and 96%, respectively, of these neurons were invested with a few to many Cx36-puncta.

Specificity characteristics of the anti-Cx36 antibodies used here for Cx36 detection in various regions of rodent brain have been previously reported (Li *et al*., 2004; Rash *et al*., 2007a,b; Curti *et al*., 2012). As found in developing mouse spinal cord (Bautista *et al*.,

2012), comparison of a field in the DLN from a wild-type adult mouse with a corresponding field in the DLN from a Cx36 knockout mouse, shows Cx36-puncta among peripherin-positive motoneurons in wild-type (Fig. 2E) and an absence of labelling for Cx36 in the knockout (Fig. 2F), indicating specificity of the anti-Cx36 antibody.

Laser scanning confocal analysis of immunofluorescence labelling for Cx36 associated with peripherin-positive motoneurons in the DMN, DLN and RDLN is shown in Fig. 3. In the DMN, the intermingled anal sphincter and bulbospongiosus motoneurons are difficult to distinguish from each other. However, as previously described (McKenna and Nadelhaft 1986), bulbospongiosus motoneurons have dendrite bundles extending medial and ventral (Fig. 3A), whereas anal sphincter motoneurons have dendrites directed dorsally traversing regions just lateral and dorsal to the central canal (Fig. 3B), as well as extending contralaterally via the commissural ventral gray matter. Labelling for Cx36 among closely packed pairs or triples of these large neurons at caudal levels of the DMN was seen in regions of apposition between their somata, as well as linearly arranged along their initial dendrites (Fig. 3A-C). At rostral levels, where slightly more ventrally located DMN motoneurons are of smaller size and are clustered in greater numbers, labelling of Cx36 was similarly distributed among peripherin-labelled neuronal somata (Fig. 3D,E), but the initial dendrites of these neurons were less distinctive and displayed fewer Cx36-puncta (not shown). In the DLN (Fig. 3F), Cx36 labelling among clustered neurons was heterogeneous, consisting of isolated, moderate sized Cx36-puncta as in DMN, as well as patches of Cx36-puncta (described below) that were fewer and smaller in DLN than DMN, and numerous very fine Cx36-puncta (Fig. 3F, double arrowheads) that were less evident in DMN. Throughout all these nuclei, immunolabelling for Cx36 had an exclusively punctate appearance, with no evidence of either punctate or diffuse intracellular labelling, as determined by confocal through focus examination of individual neurons. Further, Cx36 labelling appeared to be localized exclusively to the surface (i.e., presumably plasma membrane) of motoneuronal somata and dendrites, as deduced from displays of thick (12 μm) z-stack images in 3D and rotation of these images at all angles (Supplementary Fig. 1). Similar analysis indicated that Cx36-puncta were often localized at appositions between motoneurons, which included soma-somatic (Fig. 3G), dendro-somatic (Fig. 3H) and dendro-dendritic (Fig. 3I) appositions. At lower magnification, individual Cx36-puncta appeared to be heterogeneous in size, ranging from 0.5 to 3 μm in diameter. Larger patches of Cx36 labelling were also encountered, ranging from 5 μm in diameter to as much as 5 μm × 17 μm in diameter and length, respectively. As shown at higher magnification, the larger patches in fact consisted of clusters of Cx36-puncta (Fig. 3J, and inset), which were best viewed when captured *en face* on the surface of neurons or dendrites. These clusters were often irregular in shape and contained up to dozens of Cx36-puncta.

Vglut1-containing terminals in sexually dimorphic motor nuclei

In contrast to nearly all other motor nuclei that contained an abundance of vglut1-terminals, with a substantial proportion of Cx36-puncta associated with those terminals (Bautista *et al*., 2013b), Cx36-puncta in the sexually dimorphic motor nuclei were rarely associated with these terminals. Indeed, motoneuron somata and their initial dendrites in the DMN and DLN either totally lacked or contained only a paucity of vglut1-terminals (Fig. 1C,D,E, and 3A-C) in comparison to adjacent motor nuclei (unidentified), where these terminals were seen distributed at moderate density among peripherin-positive motoneurons (Fig. 1E). However, regions of the RDLN containing both dispersed and clustered motoneurons (Fig. 1C,3K) as well as the VN displaying moderate to low levels of Cx36-puncta also contained a scattering of these terminals, where Cx36-puncta either lacked or showed co-localization with these terminals (Fig. 3K). More generally, it also appeared that vglut1-terminals were more sparsely distributed in the intermediate laminae and in ventral horn at spinal levels

containing the sexually dimorphic nuclei than in these regions at other spinal levels (Fig. 1C).

Cx36 in sexually dimorphic nuclei at PD9 and PD15

Electrophysiological analyses of spinal cord systems in vitro is often conducted using preparations from early postnatal or juvenile animals, where viability of the systems under investigation are better preserved in reduced preparations. To provide the basis for future such studies involving electrical coupling in sexually dimorphic motor nuclei, we examined the appearance of Cx36 in these nuclei at two developmental ages, PD9 and PD15, of male rats. As is typical in spinal cord at younger ages vs. adults, labelling for Cx36 in the form of Cx36-puncta was more widely distributed throughout gray matter at PD9, including ventral horn areas outside of motor nuclei (Fig. 4A). Labelling in RDLN was similar to that in surrounding regions, while labelling in DLN was somewhat more dense, and contained coarse as well as very fine Cx36-puncta (Fig. 4B). Cx36-puncta were also present in the DMN, where they were prominent on motoneuronal somata (Fig. 4C) and dendrites (Fig. 4D). In general, motoneurons in the DLN and DMN had much smaller somata and less developed dendritic arborizations at PD9 than at PD15 or in adults, as previously reported (Goldstein *et al*., 1990; Goldstein and Sengelaub, 1993). The density of Cx36-puncta among these neurons was also far less and did not occur in tight clusters as seen at later ages. At PD15, motoneurons in each of the dimorphic nuclei were well developed, and displayed robust labelling for peripherin in their somata and widely distributed dendrites (Fig. 4D-N). Labelling for Cx36 was still seen in regions surrounding motor nuclei (Fig. 4E,F,K), but Cx36-puncta were more concentrated within DMN, DLN and RDLN than in surrounding areas. Although not examined quantitatively, several features of this labelling at PD15 differed qualitatively from patterns seen in adult rats. First, Cx36-puncta appeared to be present in greater abundance along peripherin-positive dendrites within, and extending from, the DMN, DLN and RDLN (Fig. 4E-K). The puncta often occurred along bundles of intertwined dendrites (Fig. 4H,I,J,K), including at intersections between dendrites (Fig. 4M,N), and likely represent mature rather than nascent gap junctions. Second, although Cx36-puncta were also heavily concentrated among neuronal somata in the dimorphic nuclei, these more often appear as individual puncta (Fig. 4F,G,I,J), rather than assemblies of puncta in clusters as seen in adults. Clusters of puncta were, nevertheless, encountered but far less frequently than in mature animals (Fig. 4L,M). And third, very fine Cx36-puncta barely visible at low magnification (Fig. 4G) were often seen distributed along the surface of motoneuron somata and dendrites (Fig. 4M,O). These fine puncta had diameters that were about 5-10 fold smaller than their larger counterparts, and they were not seen on motoneurons in adult animals. These results suggest that considerable remodelling of Cx36-containing gap junctions in sexually dimorphic nuclei takes place between the end of the second postnatal week and adulthood.

Cx36 in sexually dimorphic nuclei of female rat

Motoneurons in sexually dimorphic motor nuclei in female rats are present in about one-third the number, are smaller and have less extensive dendritic arborizations compared with their male counterparts (Breedlove, 1986; Sengelaub and Arnold, 1986). In males, dimorphic motoneurons in DMN and DLN innervating the dimorphic bulbospongiosus and ischiocavernosus muscles, respectively, are intermingled with non-dimorphic motoneurons innervating the anal sphincter and urethral sphincter muscles, respectively. In females, motoneurons innervating the two sphincters represent the vast majority of neurons in the DMN and DLN (McKenna and Nadelhaft, 1986). Thus, females provide the opportunity to determine whether non-dimorphic motoneurons in these nuclei express Cx36. As shown in Figure 5, both the DMN and DLN, as well as the RDLN, contained Cx36-puncta. Labelling of Cx36 was particularly striking in the DLN, which appeared smaller than its male

counterpart, but displayed a density of Cx36-puncta similar to that seen in males (Fig. 5A-C). Patterns of dispersed Cx36-puncta and patches of these puncta in regions of RDLN containing loosely arrayed motoneurons (Fig. 5D,E), as well as those at rostral levels containing more clustered motoneurons (Fig. 5F), were also similar to that seen in males. In contrast, labelling in the DMN was considerably less in females, which was not simply a consequence of the smaller and reduced number of motoneurons in this nucleus of females vs. males. Although not examined quantitatively, Cx36-puncta along initial dendritic shafts and clusters of Cx36-puncta on the somata of DM motoneurons were clearly fewer (Fig. 5G-I) than seen in males, and those clusters that were present tended to be smaller (Fig. 5H,I).

Distribution of dimorphic motoneurons in EGFP-Cx36 mice

Mice exhibit similar sexually dimorphic patterns of their lower lumbar motoneurons as observed in rats (Wee and Clemens, 1987; Forger *et al*., 1997; Zuloaga *et al*., 2007). As previously noted (Forger *et al*., 1997; Zuloaga *et al*., 2007), however, motoneurons in DMN of mice appear more dispersed and, in addition to their location at the apex of the ventral funiculus, tend to occupy areas more ventrally and laterally near the border between white and gray matter. Thus, whereas DMN and DLN are largely segregated in rat, some dimorphic motoneurons are found to be distributed between these two nuclei in mouse.

To further characterize these neurons, we examined immunolabelling for EGFP in relation to that of peripherin in the dimorphic nuclei of transgenic EGFP-Cx36 mice, in which EGFP expression on a bacterial artificial chromosome (BAC) is driven by the Cx36 promoter. Although expression of Cx36 in these mice is left intact, it was not possible to double label for EGFP and Cx36 due to the incompatibility of the strong fixation required for adequately labelling EGFP (*i.e*., 4% formaldehyde), and the loss of labelling for Cx36 with this fixation. The EGFP-Cx36 BAC mice have not been widely used as yet for studies of neurons expressing Cx36. Nevertheless, as expected based on pilot examination of these mice during their production (Nagy, unpublished observations), together with the above results showing abundant Cx36-puncta associated with dimorphic motoneurons, EGFP fluorescence (not shown) as well as immunolabelling for EGFP was detected in many though not all motoneurons in the sexually dimorphic motor nuclei. Small and medium size neuronal somata labelled for EGFP were also seen sparsely distributed in other areas of the ventral horn and moderately in the dorsal horn.

A comparison of labelling for peripherin and, in the same field, labelling for EGFP is shown in Figure 6A1 and 6A2, respectively. As in rat, labelling for peripherin clearly delineated the locations of motoneurons in the DMN, DLN and RDLN (Fig. 6A1). Labelling for EGFP was prominent in the DMN and DLN (Fig. 6A2), where both neuronal somata and their dendritic extensions were intensely labelled (Fig. 6B-D), but in the RDLN, EGFP-positive neurons ranged from very sparse to undetectable (Fig. 6A2). Detailed comparisons of labelling in matching fields of the DMN (Fig. 6E1, E2), the DLN and RDLN (Fig. 6F1,F2) and RDLN (Fig. 6G1,G2) revealed that both the DMN and DLN contained peripherin-positive neurons that were EGFP-negative, although the proportion of those that were negative was not determined quantitatively. The RDLN contained only a few ventrally located peripherin-positive neurons that were labelled for EGFP (Fig. 6G). Peripherin-positive motoneurons lacking EGFP were often well intermingled with, and in close somal apposition to, other motoneurons labelled for peripherin, as shown at higher magnification in the DLN (Fig. 6H,I). The lack of labelling for EGFP in some did not appear to be a peculiarity of peripherin detection in other than motoneurons in the dimorphic nuclei because some ChAT-positive neurons in these nuclei were similarly devoid of EGFP (not shown). In female EGFP-Cx36 mice, neurons positive for EGFP were also found in both the DMN and DLN (Fig. 6J,K,), as well as midway between these nuclei in a ventromedial region

corresponding to the area of VN (Fig. 6M). However, only a few neurons per section were encountered, and these were much smaller than observed in males and their dendrites were only weakly labelled for EGFP (Fig. 6L,M).

Discussion

The appearance of motoneurons in the sexually dimorphic motor nuclei as visualized here by their labelling for peripherin was comparable to that derived from the use of other anatomical methods (McKenna and Nadelhaft, 1986). Early ultrastructural studies of motoneurons in the lumbosacral spinal cord of cat described close appositions of their dendrites, which were considered in the context of possibly contributing to electrical interactions between these neurons (Mathews *et al*. 1971; Takahashi and Yamamoto, 1979). Following the discovery of gap junctions between sexually dimorphic motoneurons in adult rat (Matsumoto *et al*., 1988,1989), there have been only a few subsequent studies focused on this topic. Consistent with these early reports describing the localization of gap junctions at dimorphic motoneuronal somata and their initial dendrites, we found the greatest densities of Cx36-puncta at these neuronal compartments, where labelling often seen at soma-somatic, dendro-somatic and dendro-dendritic appositions almost certainly reflect localization of gap junctions. Outside of the dimorphic nuclei in regions containing extensive dendritic arborizations of dimorphic motoneurons, Cx36-puncta were far more sparsely distributed, suggesting that gap junctions may link distal dendrites of the motoneurons, but at vastly lower levels. Our results raise several points for consideration.

Connexin expression in motoneurons

Like neurons elsewhere in the developing CNS, motoneurons in an assortment of motor nuclei in rodent spinal cord are known to be electrically coupled and dye-coupled via gap junctions at early postnatal ages (Arasaki *et al*., 1984; Fulton *et al*., 1980; Walton & Navarette, 1991; Bou-Flores & Berger, 2001). There has been several reports regarding connexins expressed by motoneurons, and those connexins considered to mediate motoneuronal coupling include Cx36, Cx37, Cx40, Cx43 and Cx45 (Chang *et al*., 1999; Chang and Balice-Gordon, 2000). Multipe connexins were also reported to be expressed in trigeminal motoneurons, including Cx26, Cx32, Cx36 and Cx43 (Honma *et al*., 2004). Similarly, expression of Cx32 mRNA was reported in sexually dimorphic motoneurons of adult rats (Matsumoto *et al*., 1991,1992). However, we have found widespread association of only Cx36 with motoneurons, and Cx32 protein in dimorphic nuclei (*i.e.*, DMN, DLN) was found to be assocociated only with oligodendrocytes and along myelinated fibers (Bautista *et al*., 2013a), consistent with the ultrastructural localization of Cx32 to gap junctions formed by oligodendrocytes and not to those between neurons in spinal cord (Rash *et al*., 1998; 2001b). In contrast, the robust and consistent labelling for Cx36 observed in these two sexually dimorphic nuclei, often localized to the surface of motoneurons, was among the most stricking seen anywhere in the CNS. The results provide compeling evidence that previously described gap junctions linking these motoneurons (Matsumoto *et al*., 1988,1989) are composed of Cx36, and suggest Cx36-mediation of electrical coupling between these neurons. In analogy with recent findings surrounding the biophysical properties of electrical coupling between neurons in the mesencephalic trigeminal nucleus (Curti *et al*., 2012), the high density of Cx36-containing gap junctions linking dimorphic motoneurons might be predicted to maintain strong coupling coeficients between these cells even if only a small proportions of these channels were in an open state a any given moment.

Coupling between developing vs. adult motoneurons

The notion that gap junction-mediated coupling between neurons uniformly diminishes during development, resulting in its absence in many areas of adult CNS is no longer tenable. Despite the reported loss of motoneuronal coupling during development (Walton & Navarette, 1991), evidence for electrical coupling and presence of gap junctions has been found in several motoneuronal systems in adult animals (Gogan *et al*., 1974, 1977; Lewis, 1994; van der Want *et al*., 1998). Dendritic bundling and close somal appositions are especially prominent features of sexually dimorphic motoneurons (Schroder, 1980; McKenna and Nadelhaft, 1986; Bellinger and Anderson, 1987), and it was suggested that these appositions might be sites of direct electrical interactions (Rose and Collins, 1985). As predicted, gap junctions are especially prominent between sexually dimorphic motoneurons in the DMN and DLN in *adult* male rats (Matsumoto *et al*., 1988,1989), and such junctions have even been described between these neurons in their equivalent Onuf's nucleus in adult human spinal cord (Feirabend *et al*., 1997). Moreover, our results based on Cx36 localization indicate that these junctions increase from PD9 to PD15 and are further deployed at motoneuronal somatic appositions beyond this developmental period. In keeping with these findings, motoneurons in the DMN, DLN and RDLN of adult animals were reported to exhibit dye-coupling following injection of Neurobiotin into single motoneurons (Coleman and Sengelaub, 2002). However, these motoneurons were also found to be coupled to interneurons in these nuclei, which is unsusual as neuronal coupling in other systems typically occurs in a homologous fashsion (*i.e.*, coulping between same cell types). It should be noted that although dye-coupling in these studies was eliminated by the relatively non-specific gap junction blocker oleamide, those studies were conducted using formadehyde-fixed sections, under which the preservation of a normal physiological state of gap junctions is uncertain. Interneurons would not have been identified by the peripherin marker used in the present study, precluding possible identification of Cx36-puncta at appositions between these neurons and motoneurons. In any case, the association of dye-coupling (albeit in fixed tissues), ultrastructurally-identified gap junctions and Cx36 with sexually dimorphic adult motoneurons are all consistent with a brief report (the only one we are aware of) describing electrical coupling between these neurons in adult rat (Collins and Erichsen, 1988).

Cx36 at purely electrical vs. mixed synapses

It has previously been reported that motoneurons in the sexually dimorphic DMN and DLN, unlike those at most other spinal levels, receive very little monosynaptic primary afferent input (Jankowska *et al*., 1978; McKenna and Nadelhaft, 1986; Thor and de Groat, 2010). Because vglut1 is contained largely in axon terminals of primary afferent origin (Alvarez *et al*., 2004), our findings of a near total absence of vglut1-containing terminals on motoneuronal somata and dendrites within the DMN and DLN confirm these earlier reports. In gray matter regions surrounding these nuclei, labelling for vglut1 was far less dense than seen at other spinal levels, suggesting a paucity of vglut1-terminals also on the extensive dendritic arborizations that the dimorphic neurons have in these regions (Goldstein *et al*., 1990; Goldstein and Sengelaub, 1993). The dearth of vglut1-containing terminals on sexually dimorphic motoneurons, unlike motoneurons in other spinal cord motor nuclei, where these terminals are abundant and largely of primary afferent origin, indicates lack of a monosynaptic primary afferent influence on, or reflex control of, these motoneurons, the functional significance of which is poorly understood.

We originally examined primary afferent vglut1-containing terminals in the context of their relationship to labelling for Cx36 in the sexually dimorphic *vs*. other spinal motor nuclei. We recently reported (Bautista *et al*., 2013b) that abundant Cx36-puncta persist on the vast majority of motoneurons along the spinal axis in *adult* rat and mouse, but these puncta rarely

appeared at appositions between motoneurons. Rather, they were localized to a considerable extent at vglut1-positive primary afferent axon terminals on these neurons, forming what we deduced to be Cx36-containing gap junctions between axon terminals and postsynaptic neurons. Such structures, termed morphologically "mixed synapses" with potential for dual chemical/electrical transmission (Bennett and Goodenough, 1978), were much earlier reported to be widespread in rodent spinal cord (Rash *et al*., 1996), and have been described in other areas of the mammalian CNS, including the lateral vestibular nucleus (Korn *et al*., 1973) and hippocampus (Vivar *et al*., 2012; Hamzei-Sichani *et al*., 2012; Nagy, 2012). Gap junctions at mixed synapses are presumably incapable or less effective in the mediation of coupling between their postsynaptic cells (see however, Nagy *et al*., 2013), possibly explaining the absence of coupling between most motoneurons despite persitance of Cx36-puncta on these neurons in adult rodents. The dimorphic motor nuclei, in contrast, embody an exception where all Cx36-puncta occurring on motoneuronal somata and their initial dendrites lack association with vglut1-terminals, and where these puncta therefore may be considered to represent "purely electrical synapses". At these synapses, Cx36 occurred as isolated Cx36-puncta and as patches or clusters of closely aggregated individual Cx36-puncta. Such aggregates of puncta are not unique to the sexually dimorphic nuclei, but also occur at other locations, including at gap junctions between mesencephalic trigeminal motoneurons, mixed synapses formed in the vestibular nuclei by vestibular primary afferents and similar mixed synapses in spinal cord (Curti *et al*., 2012; Nagy *et al*., 2013; Bautista *et al*., 2013b). These aggregates may represent "hot spots" for Cx36 trafficking, where the protein machinery required for Cx36 transport, plasma membrane insertion and removal may be particularly enriched.

EGFP expression in dimorphic nuclei of EGFP-Cx36 mice

In male mice, both the DMN and DLN displayed EGFP-positive motoneurons in EGFP-Cx36 mice, consistent with detection of Cx36 protein in these nuclei. Howevre, the absence of EGFP in some peripherin-positive motoneurons in each of these nuclei suggests the presence of both gap junctionally coupled and non-coupled motoneurons. Nevertheless, our analyses in mouse revealed that, at minimum, a few Cx36-puncta were associated with nearly all peripherin-positive motoneuronal somata in the DMN and DLN. This, together with the near total absence of EGFP in the RDLN, where Cx36-puncta though sparse were clearly seen on motoneurons, raises an additional and/or alternative possibility, namely false-negative EGFP expression in Cx36-expressing cells, which may occur with incomplete BAC transgene integration (van Keuren *et al*., 2009). Further, we note that there was an absence of EGFP expression in motor nuclei lying in the vicinity of the sexually dimorphic groups (not shown), which is also in contrast to the dense distribution of Cx36-puncta associated with vglut1-terminals at mixed synapses on motoneurons in these nuclei (Bautista *et al*., 2013b). Absence of EGFP in those motoneurons receiving mixed synapses may again reflect false-negative EGFP expression or, alternatively, the existence of heterotypic gap junctions at these mixed synapses, such that primary afferent terminals contain Cx36, whereas motoneurons express another as yet unidentified connexin. Analysis of dye-coupling in the EGFP-Cx36 mice as well as ultrastructural studies in combination with immunolabelling for Cx36 will be required to distinguish between these various possibilities.

Dimorphic and non-dimorphic motoneurons in the DMN and DLN

Despite reports of gap junctions, dye-coupling and electrical coupling in sexually dimorphic nuclei discussed above, little is known about the organization of this coupling among motoneuronal populations contained in these nuclei. In males, sexually dimorphic motoneurons in the DMN and DLN are intermixed with anal sphincter and external urethral sphincter (EUS) motoneurons, respectively, which are not considered to be sexually

dimorphic because their number and size do not vary between males vs. females (McKenna and Nadelhaft, 1986). It remains unresolved whether both dimorphic and non-dimorphic motoneurons in these nuclei are coupled and, if both, whether the former are additionally coupled to the latter. Several of our observations suggest coupling of both dimorphic and non-dimorphic pools of motoneurons in both the DMN and DLN. First, the association of Cx36-puncta with nearly all peripherin-positive motoneurons in the DMN and DLN suggests that the vast majority of these neurons are gap junction communication competent. Second, the DMN contains many more motoneurons in male than in female rats (Jordan *et al*., 1982). In female rats lacking ischiocavernosus and bulbospongiosus muscles, it has been noted that motoneurons in the DMN projecting to the anal sphincter and those in DLN projecting to the EUS appear to account for all of the motoneurons in these nuclei (McKenna and Nadelhaft, 1986). The presence of Cx36-puncta at a high density in the DLN and an albeit lower density in DMN of female rats suggests coupling between EUS motoneurons and between anal sphincter motoneurons. This is further supported by the presence of EGFP-positive motoneurons in both DMN and DLN of female EGFP-Cx36 mice. And third, bulbospongiosus and anal sphincter motoneurons are highly intermingled in the DMN, while ischiocavernosus and EUS motoneurons are somewhat segregated in the DLN of rat, with the former lying medially and the latter occupying a lateral position in the nucleus (Rose and Collins, 1985; McKenna and Nadelhaft, 1986). Our finding that medially and laterally located motoneurons in DLN were equally decorated with Cx36-puncta suggests a similar capacity of coupling among the two motoneuronal pools. However, although we cannot shed light on whether the sexually dimorphic motoneurons are coupled to the sphincter motoneurons, such heteronymous coupling is likely based on observations from retrograde tracing studies that DM motoneurons that have projections to the bulbospongiosus muscle are gap junctionally coupled to those that do not project to this muscle (Matsumoto *et al*., 1988). Definitive studies to resolve this issue will require examination of dye-coupling or electrical coupling between anatomically or electrophysiologically identified EUS and simultaneously identified ischiocavernosus motoneurons in the DLN and similar examination of coupling between anal sphincter and ischiocavernosus motoneurons in the DMN.

Functional considerations

A fundamental role of electrical synapses in the mammalian brain is their promotion of synchronous activity in networks of coupled neurons. This is achieved by synchronizing subthreshold membrane oscillations so that the network may reach threshold for firing in unison following an excitatory input. Direct electrical interactions between developing spinal motoneurons was also considered to be important in driving synchronous activity of these neurons (Kiehn and Tresch, 2002). In adult rodent spinal cord, the presence of neuronal gap junctions and the synchronous neuronal activity they presumably confer among sexually dimorphic motoneurons may give rise to coupled network activity of these neurons and their target muscles. As previously discussed (Coleman & Sengelaub, 2002), this coupling could be required for production of synchronous activity of motoneurons to maintain concerted action of the constellation of perineal muscles that support the physiology and behaviour of copulation. Though Cx36 knockout mice are able to reproduce, parameters of their copulatory behavior in the absence of electrical coupling has not been examined.

In male rodents, it is generally accepted that the ischiocavernosus and bulbospongiosus muscles contribute to various parameters of sexual behavior (Hart and Melese-D'Hospital, 1983; Elmore and Sachs, 1988; Holmes *et al*., 1991; Schmidt and Schmidt 1993). Patterns of activity of these and related muscles was remarkably revealed in sexual reflexes elicited in anesthetized rats after acute spinal transection (McKenna *et al*., 1991), which was

considered to remove tonic descending inhibition of these reflexes (Marson and McKenna, 1990). The urethrogenital reflex, as it was termed, reproduced some features of copulation in the intact male, including penile erection, pelvic muscle activation and ejaculation. For plausible reasons given, this reflex could be evoked only by sensory stimulation of the urethra (McKenna *et al*., 1991). Recordings from the ischiocavernosus and bulbospongiosus muscles, as well as from the pudendal nerve innervating these two muscles and the anal and urethral sphincters, indicated that all the perineal muscle contractions were synchronous during reflex activation (McKenna *et al*., 1991), reflecting requirment of the dimporphic muscles in erectile and ejaculatory functions and, as suggested (McKenna and Nadelhaft, 1989), maintenance of tonic activity in the sphincter muscles for closure of the anal and urethral sphincters during sexual activity. We speculate that removal of tonic descending inhibition of sexual reflexes unmasks the considerable extent to which motoneurons in DMN and DLN appear to be electrically coupled, which is manifest by the observed synchronous activity of their target muscles following elicitation of the urethrogenital reflex. Further, the more complex sequelae of perineal muscle activity seen in normal male rats during sexual activity (Holmes *et al*., 1991; Schmidt and Schmidt, 1993) suggests that moment-to-moment patterns of coupling between motoneuronal pools in these nuclei may be subject to strict regulation.

Supplementary Material

Refer to Web version on PubMed Central for supplementary material.

Acknowledgments

This work was supported by a grant from the Canadian Institutes of Health Research to J.I.N. (MOP 106598), and by grants from the National Institutes of Health (NS31027, NS44010, NS44295) to JE Rash with sub-award to JIN. We thank B. McLean for excellent technical assistance, Dr. B.D. Lynn for help with genotyping EGFP-Cx36 transgenic mice, and Dr. D. Paul (Harvard University) for providing breeding pairs of Cx36 knockout and wild-type mice.

References

Alvarez FJ, Villalba RM, Zerda R, Schneider SP. Vesicular glutamate transporters in the spinal cord, with special reference to sensory primary afferent synapses. J Comp Neurol. 2004; 472:257–280. [PubMed: 15065123]

Arasaki K, Kudo N, Nakanishi T. Firing of spinal motoneurons due to electrical interactions in the rat: an in vitro study. Exp Brain Res. 1984; 54:437–445. [PubMed: 6723863]

Bautista W, Nagy JI, Dai Y, McCrea DA. Requirement of neuronal connexin36 in pathways mediating presynaptic inhibition of primary afferents in functionally mature mouse spinal cord. J Physiol. 2012; 590:3821–39. [PubMed: 22615430]

Bautista W, Nagy JI. Re-evaluation of connexin (Cx26, Cx32, Cx36, Cx37, Cx40, Cx43, Cx45) association with motoneurons in rodent spinal cord, sexually dimorphic motor nuclei and trigeminal motor nucleus. Submitted. 2013a

Bautista W, McCrea DA, Nagy JI. Connexin36 identified at morphologically mixed chemical/electrical synapses on trigeminal motoneurons and at primary afferent terminals on spinal cord neurons in adult mouse and rat. 2013b Submitted.

Bellinger DL, Anderson WJ. Postnatal development of cell columns and their associated dendritic bundles in the lumbosacral spinal cord of the rat. I. The ventrolateral cell. column Dev Brain Res. 1987; 35:55–67.

Bennett MVL, Goodenough DA. Gap junctions, electrotonic coupling, and intercellular communication. Neurosci Res Prog Bull. 1978; 16:373–485.

Bennett MVL. Gap junctions as electrical synapses. J Neurocytol. 1997; 26:349–366. [PubMed: 9278865]

Bennett MVL, Zukin SR. Electrical coupling and neuronal synchronization in the mammalian brain. Neuron. 2004; 41:495–511. [PubMed: 14980200]

Bou-Flores C, Berger AJ. Gap junctions and inhibitory synapses modulate inspiratory motoneuron synchronization. J Neurophysiol. 2001; 85:1543–1551. [PubMed: 11287478]

Breedlove SM, Arnold AP. Hormone accumulation in a sexually dimorphic motor nucleus in the rat spinal cord. Science. 1980; 210:564–566. [PubMed: 7423210]

Breedlove SM. Cellular analysis of hormone influence on motoneuronal development and function. J Neurobiol. 1986; 17:157–176. [PubMed: 3519862]

Chang Q, Balice-Gordon RJ. Gap junctional communication among developing and injured motor neurons. Brain Res Rev. 2000; 3:242–249. [PubMed: 10751674]

Chang Q, Gonzalez M, Pinter MJ, Balice-Gordon RJ. Gap junctional coupling and patterns of connexin expression among neonatal rat lumbar spinal neurons. J Neurosci. 1999; 19:10813–10828. [PubMed: 10594064]

Ciolofan C, Lynn BD, Wellershaus K, Willecke K, Nagy JI. Spatial relationships of connexin36, connexin57 and zonula occludens-1 (ZO-1) in the outer plexiform layer of mouse retina. Neuroscience. 2007; 148:473–488. [PubMed: 17681699]

Clarke WT, Edwards B, McCullagh KJ, Kemp MW, Moorwood C, Sherman DL, Burgess M, Davies KE. Syncoilin modulates peripherin filament networks and is necessary for large-calibre motor neurons. J Cell Sci. 2010; 123:2543–52. [PubMed: 20587592]

Coleman AM, Sengelaub DR. Patterns of dye coupling in lumbar motor nuclei of the rat. J Comp Neurol. 2002; 454:34–41. [PubMed: 12410616]

Collins WF III, Erichsen JT. Direct excitatory interactions between rat penile motoneurons. Abstr Soc Neurosci. 1988; 14:181.

Condorelli DF, Parenti R, Spinella F, Salinaro AT, Belluardo N, Cardile V, Cicirata F. Cloning of a new gap junction gene (Cx36) highly expressed in mammalian brain neurons. Eur J Neurosci. 1998; 10:1202–1208. [PubMed: 9753189]

Condorelli DF, Belluardo N, Trovato-Salinaro A, Mudo G. Expression of Cx36 in mammalian neurons. Brain Res Rev. 2000; 32:72–85. [PubMed: 10751658]

Connors BW, Long MA. Electrical synapses in the mammalian brain. Annu Rev Neurosci. 2004; 27:393–418. [PubMed: 15217338]

Curti S, Hoge G, Nagy JI, Pereda AE. Synergy between electrical coupling and membrane properties promotes strong synchronization of neurons of the mesencephalic trigeminal nucleus. J Neurosci. 2012; 32:4341–4359. [PubMed: 22457486]

Deans MR, Gibson JR, Sellitto C, Connors BW, Paul DL. Synchronous activity of inhibitory networks in neocortex requires electrical synapses containing connexin36. Neuron. 2001; 31:477–485. [PubMed: 11516403]

Degen J, Meier C, van der Giessen RS, Sohl G, Petrasch-Parwez E, Urschel S, Dermietzel R, Schilling K, de Zeeuw CI, Willecke K. Expression pattern of lacZ reporter gene representing connexin36 in transgenic mice. J Comp Neurol. 2004; 47:3511–525.

Elmore LA, Sachs BD. Role of the bulbospongiosus muscles in sexual behavior and fertility in the house mouse. Physiol Behav. 1988; 44:125–129. [PubMed: 3237806]

Evans WH, Martin PEM. Gap junctions: structure and function. Mol Membr Biol. 2002; 19:121–136. [PubMed: 12126230]

Feirabend HKP, Hoitsma E, Choufoer H, Ploeger S. Light and electron microscopic study of Onuf's nucleus in man: Qualitative and quantitative aspects. Eur J Morphol. 1997; 35:371.

Forger NG, Howell ML, Bengston L, MacKenzie L, DeChiara TM, Yancopoulos GD. Sexual dimorphism in the spinal cord is absent in mice lacking the ciliary neurotrophic factor receptor. J Neurosci. 1997; 17:9605–9612. [PubMed: 9391015]

Foster AM, Sengelaub DR. Bilateral organization of unilaterally generated activity in lumbar spinal motoneurons of the rat. Brain Res. 2004; 1009:98–109. [PubMed: 15120587]

Fulton BP, Miledi R, Takahashi T. Electrical synapses between motoneurons in the spinal cord of the newborn rat. Proc R Soc London Ser B. 1980; 206:115–120. [PubMed: 6105652]

Gogan P, Gueritaud JP, Horcholle-Bossavit G, Tyc-Dumont S. Electrotonic coupling between motoneurons in the abducens nucleus of the cat. Exp Brain Res. 1974; 21:139–154. [PubMed: 4373264]

Gogan P, Gueritaud JP, Horcholle-Bossavit G, Tyc-Dumont S. Direct excitatory interactions between spinal motoneurones of the cat. J Physiol. 1977; 272:755–767. [PubMed: 592213]

Goldstein LA, Kurz EM, Sengelaub DR. Androgen regulation of dendritic growth and retraction in the development of a sexually dimorphic spinal nucleus. J Neurosci. 1990; 10:935–948. [PubMed: 2319307]

Goldstein LA, Sengelaub DR. Motoneuron morphology in the dorsolateral nucleus of the rat spinal cord: Normal development and androgen regulation. J Comp Neurol. 1993; 338:588–600. [PubMed: 7510730]

Hamzei-Sichani F, Davidson KGV, Yasumura T, Janssen WGM, Wearne SL, Hof PR, Traub RD, Gutierrez R, Ottersen OP, Rash JE. Mixed electrical-chemical synapses in adult rat hippocampus are primarily glutamatergic and coupled by connexin36. Front Neuroanat. 2012; 6:1–26. [PubMed: 22291620]

Hart BL, Melese-D'Hospital PY. Penile mechanisms and the role of the striated penile muscles in penile reflexes. Physiol Behav. 1983; 31:807–813. [PubMed: 6665070]

Helbig I, Sammler E, Eliava M, Bolshakov AP, Rozov A, Bruzzone R, Monyer H, Hormuzdi SG. In vivo evidence for the involvement of the carboxy terminal domain in assembling connexin36 at the electrical synapse. Mol Cell Neurosci. 2010; 45:47–58. [PubMed: 20510366]

Holmes GM, Chapple WD, Leipheimer RE, Sachs BD. Electromyographic analysis of male rat perineal muscles during copulation and reflexive erections. Physiol Behav. 1991; 49:1235–1246. [PubMed: 1896506]

Hombach S, Janssen-Bienhold U, Söhl G, Schubert T, Bussow H, Ott T, Weiler R, Willecke K. Functional expression of connexin57 in horizontal cells of the mouse retina. Eur J Neurosci. 2004; 19:2633–2640. [PubMed: 15147297]

Honma S, De S, Li D, Shuler CF, Turman JE Jr. Developmental regulation of connexins 26, 32, 36 and 43 in trigeminal neurons. Synapse. 2004; 52:258–271. [PubMed: 15103692]

Hormuzdi SG, Filippov MA, Mitropoulon G, Monyer H, Bruzzone R. Electrical synapses: a dynamic signaling system that shapes the activity of neuronal networks. Biochem Biophys Acta. 2004; 1662:113–137. [PubMed: 15033583]

Jankowska E, Padel Y, Zarzecki P. Crossed disynaptic inhibition of sacral motoneurons. J Physiol. 1978; 285:425–444. [PubMed: 745104]

Jordan CL, Breedlove SM, Arnold AP. Sexual dimorphism and the influence of neonatal androgen in the dorsolateral motor nucleus of the rat lumbar spinal cord. Brain Res. 1982; 249:309–314. [PubMed: 7139305]

Kamasawa N, Furman CS, Davidson KGV, Sampson JA, Magnie AR, Gebhardt B, Kamasawa M, Morita M, Yasumura T, Pieper M, Zumbrunnen JR, Pickard GE, Nagy JI, Rash JE. Abundance and ultrastructural diversity of neuronal gap junctions in the OFF and ON sublaminae of the inner plexiform layer of rat and mouse retina. Neuroscience. 2006; 142:1093–1117. [PubMed: 17010526]

Kiehn O, Tresch MC. Gap junctions and motor behavior. Trends Neurosci. 2002; 25:108–115. [PubMed: 11814564]

Korn H, Sotelo C, Crepel F. Electrotonic coupling between neurons in the lateral vestibular nucleus. Exp Brain Res. 1973; 16:255–275. [PubMed: 4346867]

LeBeau FEN, Traub RD, Monyer H, Whittington MA, Buhl EH. The role of electrical signaling via gap junctions in the generation of fast network oscillations. Brain Res Bull. 2003; 62:3–13. [PubMed: 14596887]

Leslie ML, Forger NG, Breedlove SM. Sexual dimorphism and androgen effects on spinal motoneurons innervating the rat flexor digitorum brevis. Brain Res. 1991; 561:269–273. [PubMed: 1802343]

Lewis DI. Dye-coupling between vagal motoneurones within the compact region of the adult rat nucleus ambiguus, in-vitro. J Aut Nerv Syst. 1994; 47:53–58.

Li X, Olson C, Lu S, Kamasawa N, Yasumura T, Rash JE, Nagy JI. Neuronal connexin36 association with zonula occludens-1 protein (ZO-1) in mouse brain and interaction with the first PDZ domain of ZO-1. Eur J Neurosci. 2004; 19:2132–46. [PubMed: 15090040]

Li X, Kamasawa N, Ciolofan C, Olson CO, Lu S, Davidson KGV, Yasumura T, Shigemoto R, Rash JE, Nagy JI. Connexin45-containing neuronal gap junctions in rodent retina also contain connexin36 in both apposing hemiplaques, forming bi-homotypic gap junctions, with scaffolding contributed by zonula occludens-1. J Neurosci. 2008; 28:9769–89. [PubMed: 18815262]

Marson L, McKenna KE. The identification of a brainstem site controlling spinal sexual reflexes in male rats. Brain Res. 1990; 515:303–308. [PubMed: 2357567]

Matsumoto A, Arai Y, Urano A, Hyodo S. Androgen regulates gap junction mRNA expression in androgen-sensitive motoneurons in the rat spinal cord. Neurosci Lett. 1991; 131:159–162. [PubMed: 1662339]

Matsumoto A, Arai Y, Urano A, Hyodo S. Effect of androgen on the expresssion of gap junction and beta-actin mRNAs in adult rat motoneurons. Neurosci Res. 1992; 14:133–144. [PubMed: 1326732]

Matsumoto A, Arnold AP, Micevych PE. Gap junctions between lateral spinal motoneurons in the rat. Brain Res. 1989; 495:362–366. [PubMed: 2765937]

Matsumoto A, Arnold AP, Zampighi G, Micevych PE. Androgenic regulation of gap junctions between motoneurons in the rat spinal cord. J Neurosci. 1988; 8:4177–4138. [PubMed: 3183718]

Matthews MA, Willis WD, Williams V. Dendrite bundles in lamina IX of cat spinal cord: a possible source for electrical interaction between motoneurons? Anat Rec. 1971; 171:313–328. [PubMed: 4939720]

McKenna KE, Nadelhaft I. The organization of the pudendal nerve in the male and female rat. J Comp Neurol. 1986; 248:532–549. [PubMed: 3722467]

McKenna KE, Nadelhaft I. The pudendo-pudendal reflex in male and female rats. J Aut Ner Syst. 1989; 27:67–77.

McKenna KE, Chung SK, McVary KT. A model for the study of sexual function in anesthetized male and female rats. Am J Physiol. 1991; 261:1276–85.

Meier C, Dermietzel R. Electrical synapses--gap junctions in the brain. Results Probl Cell Differ. 2006; 43:99–128. [PubMed: 17068969]

Nagy JI, Dudek FE, Rash JE. Update on connexins and gap junctions in neurons and glia in in the mammalian central nervous system. Brain Res Rev. 2004; 47:191–215. [PubMed: 15572172]

Nagy JI. Evidence for connexin36 localization at hippocampal mossy fiber terminals suggesting mixed chemical/electrical transmission by granule cells. Brain Res. 2012; 1487:107–122. [PubMed: 22771400]

Nagy JI, Bautista W, Blakley B. Morphologically mixed chemical-electrical synapses in developing and adult rodent vestibular nuclei as revealed by immunofluorescence detection of connexin36 and vesicular glutamate transporter-1. Neuroscience. 2013; 252:468–488. [PubMed: 23912039]

Nicolopoulos-Stournaras S, Iles JF. Motor neuron columns in the lumbar spinal cord of the rat. J Comp Neurol. 1983; 217:75–85. [PubMed: 6875053]

Rash JE, Dillman RK, Bilhartz BL, Duffy HS, Whalen LR, Yasumura T. Mixed synapses discovered and mapped throughout mammalian spinal cord. Proc Natl Acad Sci. 1996; 93:4235–4239. [PubMed: 8633047]

Rash JE, Yasumura T, Dudek FE. Ultrastructure, histological, distributio n, and freeze-fracture immunocytochemistry of gap junctio ns in rat brain and spinal cord. Cell Biol Int. 1998; 22:731–749. [PubMed: 10873288]

Rash JE, Staines WA, Yasumura T, Pate D, Hudson CS, Stelmack GL, Nagy J. Immunogold evidence that neuronal gap junctions in adult rat brain and spinal cord contain connexin36 (Cx36) but not Cx32 or Cx43. Proc Natl Acad Sci. 2000; 97:7573–7578. [PubMed: 10861019]

Rash JE, Yasumura T, Dudek FE, Nagy JI. Cell-specific expression of connexins, and evidence for restricted gap junctional coupling between glial cells and between neurons. J Neurosci. 2001a; 21:1983–2000. [PubMed: 11245683]

Rash JE, Yasumura T, Davidson K, Furman CS, Dudek FE, Nagy JI. Identification of cells expressing Cx43, Cx30, Cx26, Cx32 and Cx36 in gap junctions of rat brain and spinal cord. Cell Commun Adhes. 2001b; 8:315–320. [PubMed: 12064610]

Rash JE, Pereda A, Kamasawa N, Furman CS, Yasumura T, Davidson KGV, Dudek FE, Olson C, Nagy JI. High-resolution proteomic mapping in the vertebrate central nervou system: Close proximity of connexin35 to NMDA glutamate receptor clusters and co-localization o connexin36 with immunoreactivity for zonula occludens protein-1 (ZO-1). J Neurocytol. 2004; 33:131–152. [PubMed: 15173637]

Rash JE, Olson CO, Davidson KGV, Yasumura T, Kamasawa N, Nagy JI. Identification of connexin36 in gap junctions between neurons in rodent locus coeruleus. Neuroscience. 2007a; 147:938–956. [PubMed: 17601673]

Rash JE, Olson CO, Pouliot WA, Davidson KGV, Yasumura T, Furman CS, Royer S, Kamasawa N, Nagy JI, Dudek FE. Connexin36 vs connexin32, “miniature” neuronal gap junctions, and limited electrotonic coupling in rodent suprachiasmatic nucleus. Neuroscience. 2007b; 149:350–371. [PubMed: 17904757]

Rose RD, Collins WF. Crossing dendrites may be a substrate for synchronized activation of penile motoneurons. Brain Res. 1985; 337:373–377. [PubMed: 4027579]

Schmidt MH, Schmidt HS. The ischiocavernosus and bulbospongiosus muscles in mammalian penile rigidity. Sleep. 1993; 16:171–183. [PubMed: 8446838]

Schroder HD. Organization of the motoneurons innervating the pelvic muscles of the male rat. J Comp Neurol. 1980; 192:567–587. [PubMed: 7419745]

Sengelaub DR, Arnold AP. Development and loss of early projections in a sexually dimorphic rat spinal nucleus. J Neurosci. 1986; 6:1613–1620. [PubMed: 3711999]

Sengelaub DR, Forger NG. The spinal nucleus of the bulbocavernosus: Firsts in androgen-dependent neural sex differences. Horm Behav. 1986; 53:596–612. [PubMed: 18191128]

Senkowski D, Schneider TR, Foxe JJ, Engel K. Crossmodal binding through neural coherence: implications for multisensory processing. Trends Neurosci. 2008; 31:401–409. [PubMed: 18602171]

Singer W. Neuronal synchrony: a versatile code for the definition of relations? Neuron. 1999; 24:49–65. [PubMed: 10677026]

Söhl G, Degen J, Teubner B, Willecke K. The murine gap junction gene connexin36 is highly expressed in mouse retina and regulated during brain development. FEBS Lett. 1998; 428:27–31. [PubMed: 9645468]

Söhl G, Odermatt B, Maxeiner S, Degen J, Willecke K. New insights into the expression and function of neural connexins with transgenic mouse mutants. Brain Res Rev. 2004; 47:245–259. [PubMed: 15572175]

Söhl G, Maxeiner S, Willecke K. Expression and functions of neuronal gap junctions. Nat Rev Neurosci. 2005; 6:191–200. [PubMed: 15738956]

Takahashi K, Yamamoto T. Ultrastructure of the cell group X of Onuf in the cat sacral spinal cord. Z Mikrosk Anat Forcsh. 1979; 93:244–256.

Taylor DCM, Korf HW, Pierau FrK. Distribution of sensory neurones of the pudendal nerve in the dorsal root ganglia and their projection to the spinal cord. Cell Tiss Res. 1982; 226:555–564.

Thor KB, de Groat WC. Neural control of the female urethral and anal rhabdosphinters and pelvic floor muscles. Am J Physiol Regul Integr Comp Physiol. 2010; 299:R416–R438. [PubMed: 20484700]

Ueyama T, Arakawa H, Mizuno N. Central distribution of efferent and afferent components of the pudendal nerve in rat. Anat Embryol. 1987; 177:37–49. [PubMed: 3439636]

van der Want JJL, Gramsbergen A, Ijema-Paassen J, de Weerd H, Liem RSB. Dendro-dendritic connections between motoneurons in the rat spinal cord: an electron microscopic investigation. Brain Res. 1998; 779:342–345. [PubMed: 9473719]

Van Keuren ML, Gavrillina GB, Filipiak WE, Zeidler MG, Saunders TL. Generating transgenic mice from bacterial artificial chromosomes: transgenesis efficiency, integration and expression outcomes. Transgenic Res. 2009; 18:769–785. [PubMed: 19396621]

Vivar C, Traub RD, Gutierrez R. Mixed electrical–chemical transmission between hippocampal mossy fibers and pyramidal cells. Eur J Neurosci. 2012; 35:76–82. [PubMed: 22151275]

Walton KD, Navarette R. Postnatal changes in motoneurone electronic coupling studied in the in vitro rat lumbar spinal cord. J Physiol. 1991; 433:283–305. [PubMed: 1668753]

Watson, C.; Paxinos, G.; Kayalioglu, G. The spinal cord; A Christopher and Dana Reeve Foundation Text and Atlas. Academic Press; Amsterdam: 2009.

Wee BEF, Clemens LG. Characteristics of the spinal nucleus of the bulbocavernosus are influenced by genotype in the house mouse. Brain Res. 1987; 424:305–310. [PubMed: 3676829]

Wellershaus K, Degen J, Deuchars J, Theis M, Charollais A, Caille D, Gauthier B, Janssen-Bienhold U, Sonntag S, Herrera P, Meda P, Willecke K. A new conditional mouse mutant reveals specific expression and functions of connexin36 in neurons and pancreatic beta-cells. Exp Cell Res. 2008; 314:997–1012. [PubMed: 18258229]

Whittington MA, Traub RD. Interneuron diversity series: inhibitory interneurons and network oscillations in vitro. Trends Neurosci. 2003; 26:676–682. [PubMed: 14624852]

Zuloaga DG, Morris JA, Monks DA, Breedlove SM, Jordan CL. Androgen-sensitivity of somata and dendrites of spinal nucleus of the bulbocavernosus (SNB) motoneurons in male C57BL6J mice. Horm Behav. 2007; 51:207–212. [PubMed: 17126837]

Abbreviations

CNS	central nervous system
ChAT	choline acetyltransferase
Cx36	connexin36
DLN	dorsolateral nucleus
DMN	dorsomedial nucleus
EGFP	enhanced green fluorescent protein
L	lumbar
PBS	phosphate-buffered saline
RDLN	retrodorsolateral nucleus
TBS	50 mM Tris-HCl, pH 7.4, 1.5% NaCl
TBSTr	TBS containing 0.3% Triton X-100
T	thoracic
vglut1	vesicular glutamate transporter-1

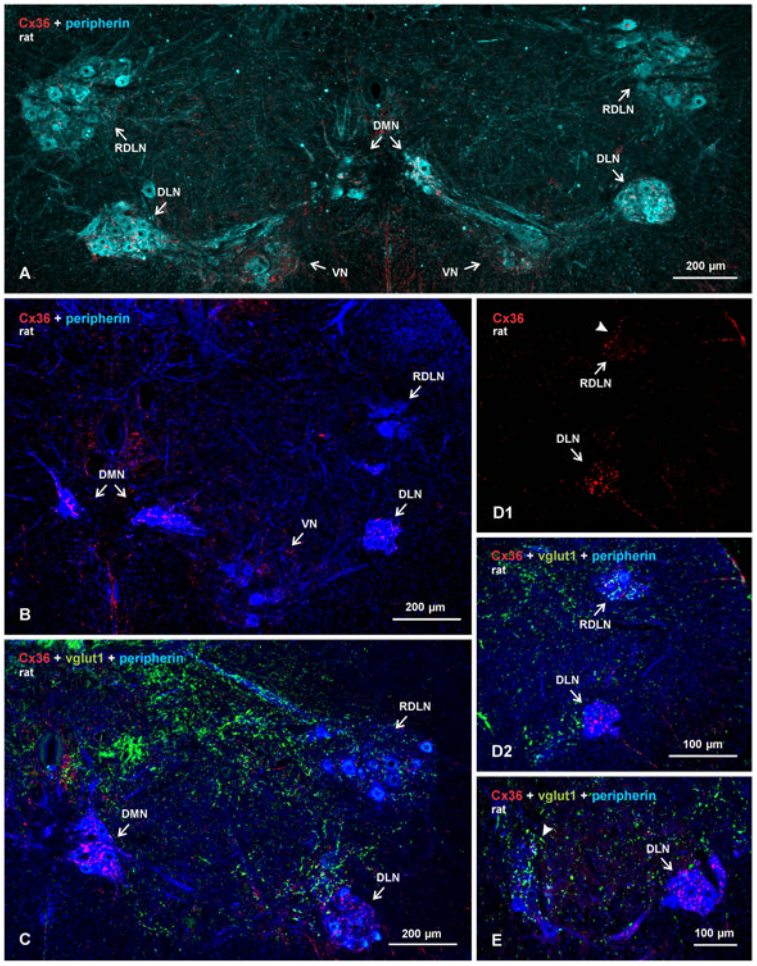

Fig. 1.

Overview of sexually dimorphic motor nuclei in relation to immunofluorescence labelling for Cx36 and vglut1 in transverse spinal cord sections of adult male rat. Motoneurons are labelled for peripherin, pseudo colored sky blue to better visualize motor nuclei (A), or deep blue to better visualize Cx36 and vglut1 (B-E). (A) Bilateral view at a lower lumbar level showing locations of, and labelling for Cx36 in, the DMN, DLN, RDLN and VN. (B-E) Images showing relative densities of labelling for Cx36 and/or vglut1, with dense labelling in the DMN and DLN (B-D) and moderate labelling in the VN (B). Sparse labelling is seen in the RDLN, as shown at a caudal level (C) and a more rostral level (D), with labelling for Cx36 shown alone (D1, arrowhead) and after overlay with labelling for peripherin and vglut1 (D2). Labelling for vglut1 is largely absent in the DMN and DLN (C,D2), and is of moderate density in the RDLN (C,D2). (E) Comparison of the absence of vglut1-terminals in DLN (arrow) vs. their presence in an adjacent unidentified motor nucleus (arrowhead).

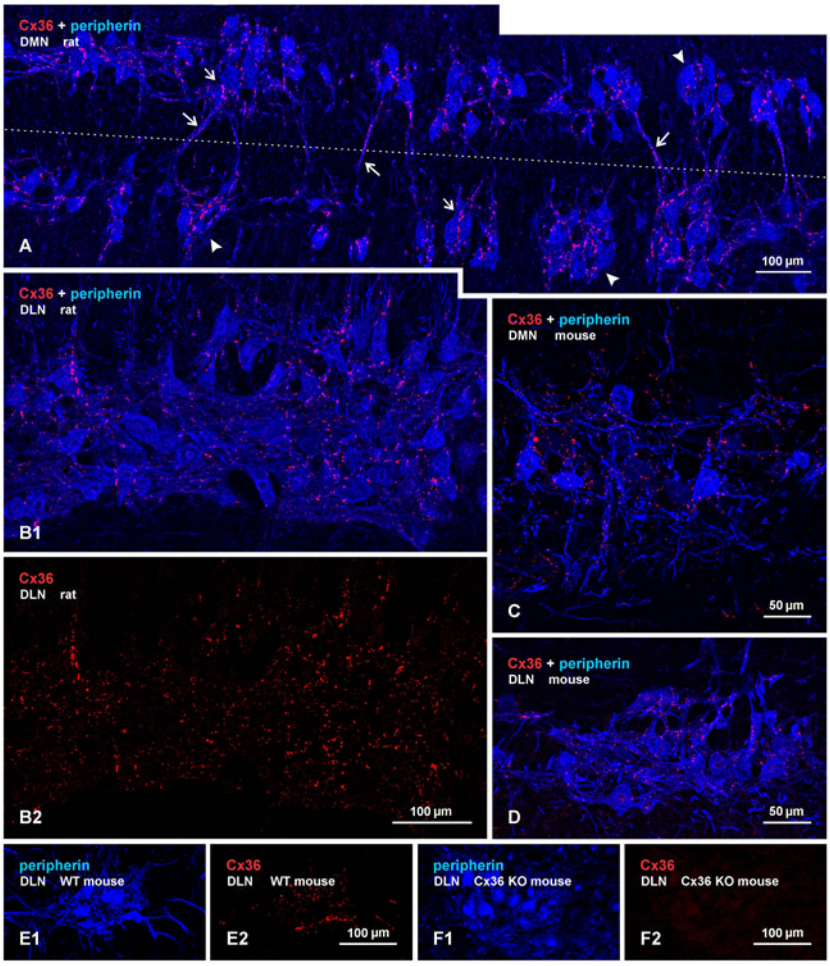

Fig. 2.

Immunofluorescence labelling of Cx36 in association with peripherin-positive motoneurons in horizontal sections through the DMN and DLN of adult rat and mouse. (A) The DMN in rat, showing intermittent clusters of motoneurons (arrowheads), with some of these neurons having contralaterally projecting dendrites. Midline is shown by dotted line. Cx36-puncta are seen densely concentrated along appositions between motoneuronal somata in the clusters (small arrows) and along bundles of intermingled dendrites spanning the midline (large arrows). (B1,B2) The same field of the DLN in rat, showing overlay of labelling for peripherin and Cx36 (B1), where Cx36-puncta are seen associated with nearly all motoneurons, and labelling for Cx36 alone (B2), where a similar density of Cx36-puncta is seen in the medial (lower half of field) and lateral (upper half of field) portions of the nucleus containing ischiocavernosus and urethral sphincter motoneurons, respectively. (C,D) The DMN (C) and DLN (D) in adult mouse, showing in each nucleus a similarly large proportion of motoneurons invested with Cx36-puncta as seen in rat. (E,F) Images of the DLN from a wild-type mouse showing the same field labelled for peripherin and Cx36 (E1,E2), and from a Cx36 knockout mouse showing the same field with absence of Cx36 among peripherin-positive motoneurons (F1,F2).

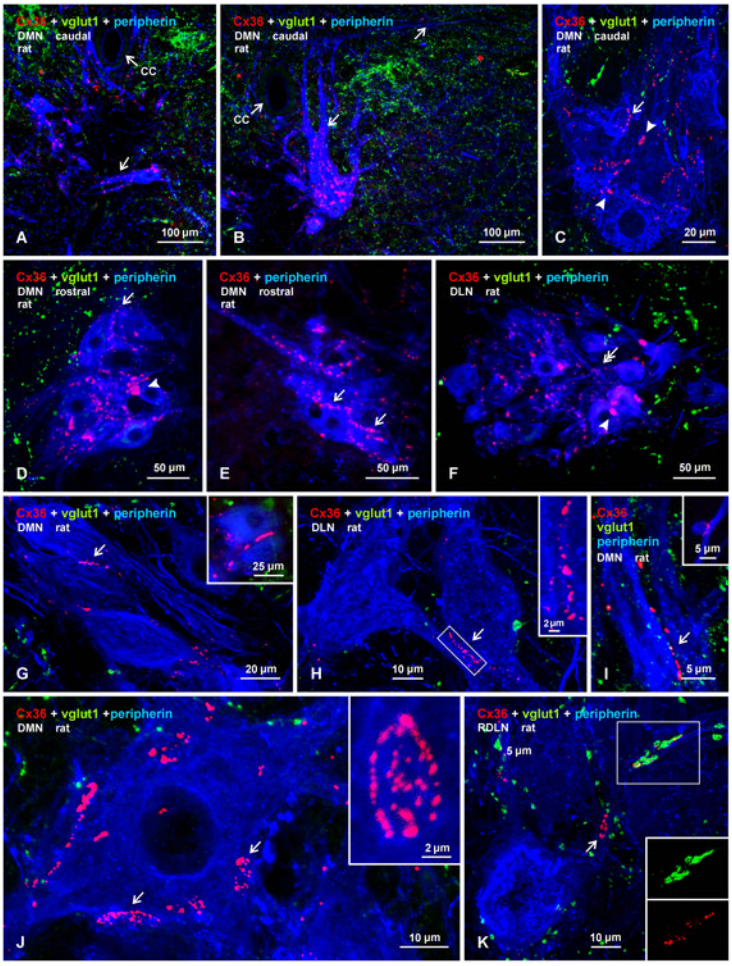

Fig. 3.

Confocal triple immunofluorescence demonstrating patterns of Cx36-puncta and vglut1-terminals associated with motoneurons in DMN, DL, and RDLN in transverse sections of adult male rat spinal cord. (A,B) Images at a caudal level of the DMN, showing closely apposed peripherin-positive motoneurons, with Cx36-puncta lining dendrites directed either horizontally across the midline (A, arrow) or directed dorsally and laterally (B, arrows) in the vicinity of the central canal (cc). (C-F) Magnifications of clusters of motoneuron somata in the caudal DMN (C), rostral DMN (D,E) and DLN (F), showing punctate appearance of labelling for Cx36 and absence of diffuse intracellular labelling for Cx36. Also evident are both large heterogeneously sized patches of Cx36 immunofluorescence (C,D, arrowheads), fine dispersed Cx36-puncta (F, double arrows), and Cx36-puncta localized around the periphery of motoneurons (single arrows). (G-I) Images of the DMN, showing Cx36-puncta localized at soma-somatic (G, arrow; also shown in inset), dendro-somatic (H, arrow; boxed area magnified in inset), and dendro-dendritic (I, arrow; and inset) appositions between peripherin-positive motoneurons. (J) Magnification of a peripherin-positive motoneuron in the DMN, showing large patches of labelling for Cx36 (arrows), consisting of clusters of individual Cx36-puncta (one cluster shown in inset). (K) Magnification of the RDLN, showing sparse distribution of vgut1-terminals among motoneurons, and Cx36-puncta with (boxed area, shown separately as green and red labels in inset) and without (arrow) co-localization at vglut1-terminals. All other images (A-J) show only occasional association of vglut1-terminals with the somata or initial dendrites of peripherin-positive motoneurons.

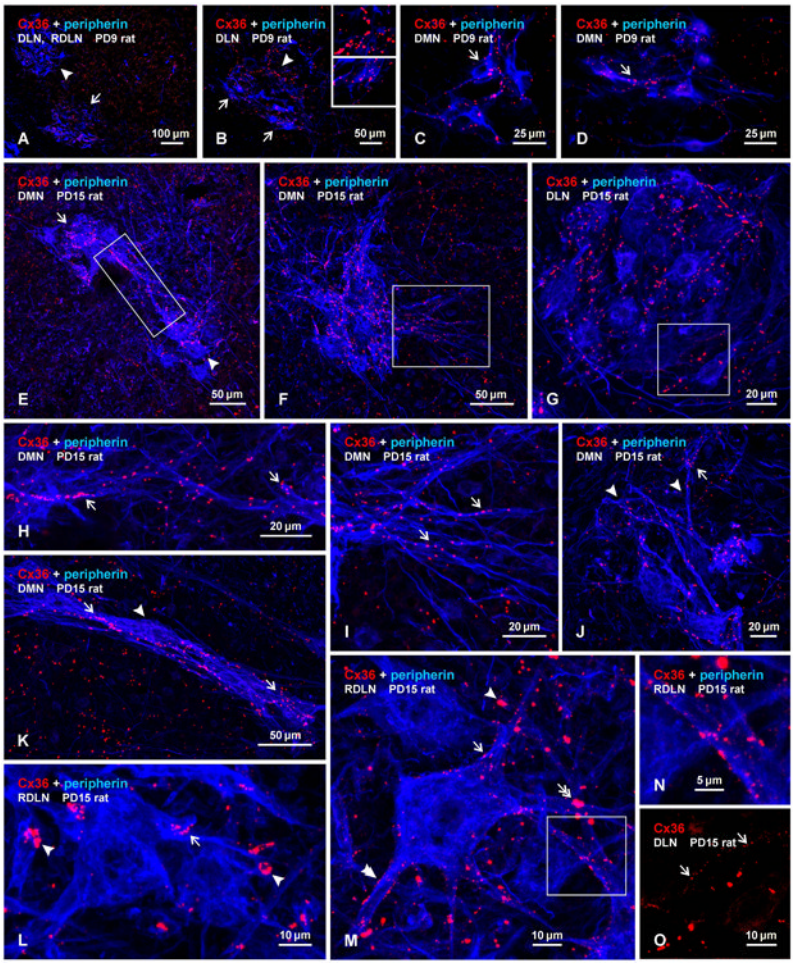

Fig. 4.

Immunofluorescence labelling of Cx36 associated with peripherin-positive motoneurons in the DMN, DLN and RDLN in transverse sections of male rat spinal cord at PD9 (A-D) and PD15 (E-O). (A-D) At PD9, Cx36-puncta are seen throughout the ventral horn, with moderate levels in the RDLN (A, arrowhead) and slightly higher concentrations in the DLN (A, arrow), which contains both coarse puncta more concentrated in the dorsomedial region (B, arrowhead; magnified in upper inset) and fine puncta more concentrated in the ventrolateral region (B, arrows; magnified in lower inset). Low levels of Cx36-puncta are seen in the DMN in association with neuronal somata (C, arrow) and dendrites (D, arrow). (E-G) Low magnifications showing labelling for Cx36 in the DMN and DLN at PD15. Clusters of motoneurons located dorsally (E, arrow) and ventrally (E, arrowhead) at a rostral level of the DMN display intermingling of their dendrites (E, boxed area), and a similar cluster at a more caudal level displays numerous laterally directed dendrites (F, boxed area). Cx36-puncta are densely distributed in the DMN (E,F) and DLN (G), and moderately in regions surrounding the DMN (E,F). (H,I) Magnifications of the boxed areas in E and F, respectively, showing Cx36-puncta among intermingled dendrites emerging from clusters of motoneurons (H, arrows), and puncta among laterally directed dendrites (I, arrows). (J,K) Images of DMN motoneurons with dorsally directed dendrites (J, arrowheads) and with a thick bundle of dendrites traversing ventrolaterally (K, arrowhead), showing Cx36-puncta along proximal as well as more distal dendritic segments (arrows). (L-N) Images of the RDLN, showing Cx36-puncta dispersed (L,M, single arrows) and in patches (L,M, single arrowheads) on motoneuron somata and dendrites, and Cx36-puncta at points of dendritic

intersections (M, double arrow and boxed area in M, magnified in N). Also evident are very fine puncta on dendrites and neuronal somata (M, double arrowhead). (O) Image showing very fine Cx36-puncta (arrows) on neuronal somata in the DLN, shown with labelling for Cx36 alone (magnified from the box area in G).

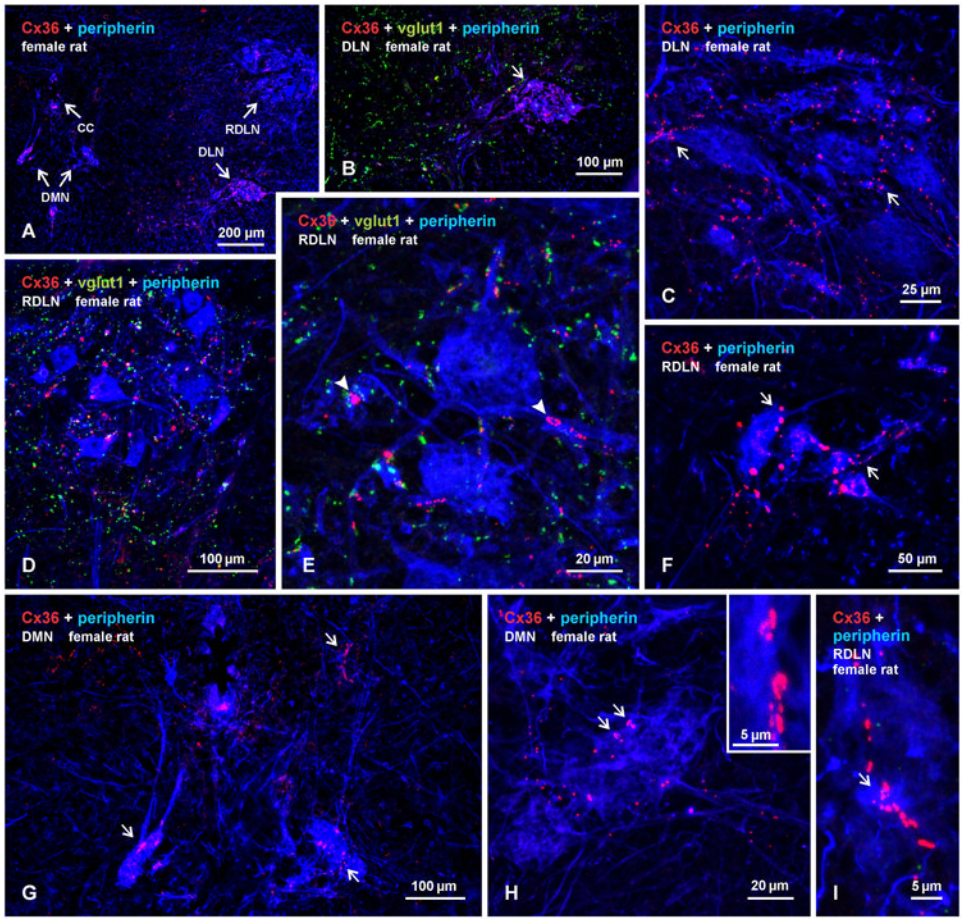

Fig. 5.

Immunofluorescence labelling of Cx36 associated with peripherin-positive motoneurons in the DMN, DLN and RDLN in transverse sections of adult female rat spinal cord. (A) Low magnification showing presence of Cx36-puncta within each of the nuclei (DMN, shown bilaterally). (B,C) Higher magnifications of the DLN, showing densely concentrated Cx36-puncta (B, arrow), absence of labelling for vglut1 (B), and association of Cx36-puncta with motoneuronal somata and dendrites (C, arrows). (D,E) Images of dispersed motoneurons in the RDLN at a caudal level, showing moderate levels of Cx36-puncta and vglut1-positive terminals within the nucleus (D), and higher magnification showing presence of patches of Cx36-puncta associated with peripherin-positive somata and dendrites (E, arrowheads), where they largely lack co-localization with vglut1-terminals. (F) The RDLN at a more rostral level, showing a diminutive cluster of small motoneurons decorated with moderate levels of Cx36-puncta (arrows). (G) Magnification of the DMN from (A), showing a few motoneurons with small somata, thin and short dendrites, and a sparse distribution of Cx36-puncta. (H,I) Magnification of the DMN and RDLN, showing sparse Cx36-puncta, and patches of Cx36-puncta (arrows, shwow also in H, inset) along peripherin-positive dendrites.

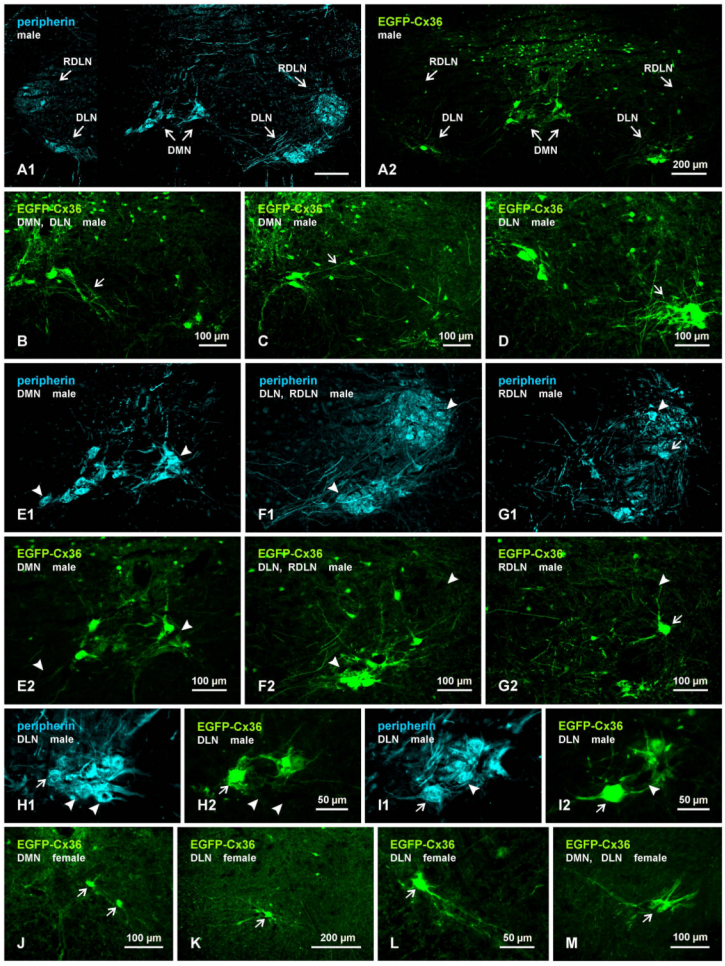

Fig. 6.

Immunofluorescence labelling of EGFP and peripherin in motoneurons of the DMN, DLN and RDLN in spinal cord of adult male (A-G) and female (J-M) EGFP-Cx36 mice in which EGFP expression on a bacterial artificial chromosome is driven by the Cx36 promoter. (A) Low magnification showing the distribution of labelling for EGFP (A1) and, in the same field, the distribution of peripherin (A2) in the DMN, DLN and RDLN. (B-D) Images of EGFP-positive motoneurons in the DMN, showing dendritic arborizations directed ventrally (B, arrow) and laterally (C, arrow), and clustering of motoneurons and dendrites in the DLN (D, arrow). (E-G) Pairs of images (E1,E2), (F1,F2) and (G1,G2) showing the same field in each pair labelled for either peripherin (E1,F1,G1) or EGFP (E2,F2,G2). In each pair, many peripherin-positive motoneurons in the DMN and DLN are also EGFP-positive, but most though not all (G, arrow) of those in RDLN and a few of those in the DMN and DLN are negative for EGFP (arrowheads). (H,I) Higher magnifications of similar pairs of images as in (E-G), showing examples of peripherin-positive motoneurons either labelled (arrows) or unlabelled (arrowheads) for EGFP. (J-M) Images from spinal cord of EGFP-Cx36 female mice, showing only a few EGFP-positive motoneurons per section in the DMN (J, arrows), DLN (K, arrow), and in a region midway between the DMN and DLN (M), and showing the smaller size of these neurons (L,M, arrrows) than seen in males (labelling for peripherin not shown).